J Appl Phycol (2017) 29:3221–3234
DOI 10.1007/s10811-017-1185-4

Competitive algal biosorption of Al^{3+}, Fe^{3+}, and Zn^{2+} and treatment application of some industrial effluents from Borg El-Arab region, Egypt

Abd El-Salam M. Shaaban[1] · Reham K. Badawy[2] · Hoda A. Mansour[1] · Mohamed E. Abdel-Rahman[3] · Yasmin I. E. Aboulsoud[2]

Received: 17 December 2016 / Revised and accepted: 30 May 2017 / Published online: 6 July 2017

Abstract Three marine algal biomasses, namely *Gelidium latifolium* (Grev.) Bornet et Thuret, *Ulva lactuca* Linnaeus and *Colpomenia sinuosa* (Mertens et Roth) Derbes et Solier, were used in their raw dried forms to biosorb Al^{3+}, Fe^{3+}, and Zn^{2+} from aqueous solutions. The optimum biosorption conditions were initial element concentration, 1000 mg L^{-1}; temperature, 40 °C; contact time, 1 h; pH, 4, 3, and 6 for Al^{3+}, Fe^{3+}, and Zn^{2+}, respectively. The highest biosorption efficiency reached 63.78, 65.95, and 111.57 mg g^{-1} for Al^{3+}, Fe^{3+}, and Zn^{2+}, respectively, using the brown algal biomass *C. sinuosa*. Examination of algal biomass surface using SEM showed several morphological changes in the cell wall surface due to biosorption such as rupturing, wrinkling, some cavity appearance, protuberance, and roughness as well as each algal type had a unique surface structure in its raw form. FTIR was used to characterize algal biomasses, and the contributing groups were variable according to heave metals and algal type as well. The thermodynamic studies revealed that the biosorption was nonspontaneous, endothermic, and chemical in nature. Freundlich isotherm model fitted slightly better than the Langmuir model in case of Zn^{2+} biosorption; meanwhile, Langmuir model fitted better in case of trivalent Al^{3+} and Fe^{3+}. The algal biomasses were efficiently regenerated and reused for four cycles via 0.01 M Na_2EDTA. Algal biomasses were applied under the optimum concluded conditions to treat 21 actual polluted industrial effluents from Borg El-Arab region, Egypt. The removal efficiency reached 80.81, 38.25, 91.79, 59.96, 95.33, 98.54, 27.39, 88.42, 36.59, and 96.98% for Al, Co, Cr, Cu, Fe, Mn, Mo, Ni, V, and Zn, respectively.

Keywords Biosorption · Marine algal biomasses · Heavy metals · Industrial effluents · Borg El-Arab city

✉ Hoda A. Mansour
rodynarwan@yahoo.com

[1] Faculty of Science, Botany Department, Ain Shams University, Cairo, Egypt

[2] Plant Ecology and Range Department, Desert Research Center, Cairo, Egypt

[3] Soil Chemistry and Physics Department, Desert Research Center, Cairo, Egypt

Introduction

Industrial wastewater is one of the important pollution sources for the aquatic environment. During the last century, a huge amount of industrial wastewater was discharged into rivers, lakes, and coastal areas. This has resulted in serious pollution problems in the aquatic environment and caused negative effects to the eco-system and human life (Aboulsoud 2008). Heavy metal pollution has become a global issue of concern due to their higher toxicities, nature of non-biodegradability, high capabilities in bioaccumulation in human body and food chain, and carcinogenicities to humans (He and Chen 2014).

In general, heavy metals are introduced into water streams as a result of mining operations, refining ores, sludge disposal, fly ash from incinerators, processing of radioactive materials, metal plating, or the manufacture of electrical equipment, paints, alloys, batteries, pesticides, or preservatives (Ahalya et al. 2003). On the other hand, heavy metals are sometimes naturally found in water resources. Growing attention is being given to the potential health hazard presented by heavy metals to the environment. Many heavy metals have chronic ill-health effects on human particularly children, such as lung tumors, allergic dermatitis, chronic bronchitis, irritation of nose, mouth and eyes, headache, stomachache, dizziness,

and diarrhea (Sud et al. 2008). Increasing environmental awareness and stringent government regulations have made the treatment of industrial wastewater mandatory. Further, if valuable, effective recovery of such heavy metals is indeed the need of the hour (Shukla and Shukla 2013).

Biosorption is a term that describes the removal of pollutants by the passive binding to biological biomass from an aqueous solution (Davis et al. 2003). Biosorption process has several possible mechanisms taking place essentially in the cell wall such as physical and chemical adsorption, electrostatic interaction, ion exchange, complexation, chelation, and microprecipitation (Aksu 2005).

The objectives of this paper were firstly, determining the optimum conditions to biosorb Al^{3+}, Fe^{3+}, and Zn^{2+} from aqueous solutions via batch biosorption using three different Egyptian algal biomasses; secondly, application of the optimum conditions in the treatment of actual polluted industrial effluents collected from Borg El-Arab region.

Materials and methods

Marine algal biomasses were collected from Abou-Keer and Almontazah shores, Alexandria (Egyptian Mediterranean Sea) during April, 2013. The algal taxa were identified and classified according to Aleem (1993) and Zinova (1967). In the field, the collected algae were immediately washed with the surrounding water to remove extraneous matter, sand particles, epiphytes, and water squeezed out. In the laboratory, the algal biomasses were washed several times with distilled water prior to air drying.

Biosorption experiments (batch procedures)

Single and multi-metal solutions were prepared by dissolving metallic salts in demineralized water. The used salts $ZnSO_4 \cdot 7H_2O$, $FeCl_3$, and $Al_2(SO_4)_3 \cdot (NH_4)_2SO_4 \cdot 24H_2O$ were analytical grade (AR) reagents purchased from Aldrich Chemical Company, Germany.

All batch experiments were carried out in triplicate. Unless otherwise stated, 0.025 g of algal biomass was put in contact with 25 mL of metal aqueous solution at room temperature for 1 h. The solution was then filtered, and the remained metal concentration was analyzed using Inductively Coupled Argon Plasma, iCAP 6500 Duo (Thermo Scientific, England). Multi-element certified standard solution of 1000 mg L^{-1} (Merck, Germany) was used as stock solution for instrument standardization. pH of the heavy metal solutions was adjusted using pH meter by addition of dilute solutions of HCl and NaOH. The maximum pH was 4, 3, and 6 for Al^{3+}, Fe^{3+}, and Zn^{2+}, respectively, as metal precipitation as hydroxides occurred at higher pH.

For the reusability and regeneration experiment, the metal-loaded algal biomass was separated by filtration, air-dried, and put in contact with a known Na_2EDTA volume. The algal biomass was separated, thoroughly washed with demineralized water, and dried prior to reuse in a new metal removal cycle.

Calculations and data evaluation

(a) The amount of biosorbed element to algal biomass was expressed according to Vitor and Corso (2008) and Kumar et al. (2005):

$$q_1 = [(C_i - C_f)\ V]/M$$

$$q_2 = [(C_i - C_f)/C_i]\ \times 100$$

where q_1 is the amount of sorbed element onto the unit amount of the biomass (mg g^{-1}), C_i is the initial concentration of element in aqueous solution (mg L^{-1}), C_f is the final (remaining) concentration of element in aqueous solution (mg L^{-1}), V is the volume of element aqueous solution (L), M is the biomass weight (g), and q_2 is the amount of removed element from the aqueous solution (%).

(b) In biosorption isotherm modeling, the linearized Langmuir and Freundlich adsorption isotherms were applied according to Salima et al. (2013) and Farah and El-Gendy (2013) where

$$C_e/q_e = 1/(Q_e K_L) + (1/Q_e)\ C_e$$

C_e is the element concentration in aqueous solution at equilibrium (mg L^{-1}), q_e is the experimental amount of adsorbed element at equilibrium (mg g^{-1}), Q_e is the calculated amount of adsorbed element at equilibrium (mg g^{-1}), and K_L is the Langmuir constant indicating the adsorption affinity of the binding sites (L mg^{-1}). By plotting C_e/q_e versus C_e, Q_e and K_L can be determined from the slope and intercept of the obtained straight line, respectively.

Whereas the linearized logarithmic Freundlich equation assumes as follows:

$$\text{Log}\ q_e = \text{Log}\ K_F + (1/n)\ \text{Log}\ C_e$$

where K_F is the Freundlich constant indicating adsorption capacity, n is the Freundlich constant indicating adsorption intensity. By plotting $Log\ q_e$ versus $Log\ C_e$, n and K_F can be determined from the slope and intercept of the obtained straight line, respectively.

(c) The thermodynamic parameters such as changes in standard free energy (ΔG), enthalpy (ΔH), and entropy (ΔS)

are determined by using the following equations according to Farah and El-Gendy (2013) and Saibaba and King (2013), where

$$K_c = C_a/C_e$$

$$\ln K_c = (-\Delta H/R).(1/T) + \Delta S/R \text{ and } \Delta G = \Delta H - \Delta S T$$

K_c is the equilibrium constant, C_a is the adsorbed element "initial concentration-final concentration" (mg L^{-1}), C_e is the remained "final concentration" (mg L^{-1}), ΔH is the change in enthalpy "heat content" (J mol^{-1}), R is the gas constant (8.314 J mol^{-1} K^{-1}), T is the temperature (K), ΔS is the change in entropy "randomness" (J mol^{-1} K^{-1}), and ΔG is the change in Gibbs' free energy of element removal (J mol^{-1}). The ΔH and ΔS values can be obtained from the slope and intercept, respectively, of the Van't Hoff plots of $ln\ K_c$ versus $1/T$. Meanwhile, ΔG values are calculated based on ΔH and ΔS values.

(d) The amount of desorbed element from algal biomass (deloaded) using disodium ethylene diamine tetra acetate (Na_2EDTA) was expressed according to Bulgariu and Bulgariu (2014) and Kanwal et al. (2013), where Desorption % = $(q_{desorbed}/q_{sorbed}) \times 100$

(e) The amount of resorbed element to algal biomass (reloaded) was expressed according to Aboulsoud (2008), where Resorption % = $(q_{resorbed}/q_{sorbed}) \times 100$

Examination of algal surface by scanning electron microscopy

The dried algal samples (raw and elements loaded biomasses) were coated by gold sputter coater (SPI-Module). The coated samples were examined by Scanning Electron Microscope (JSM-5500 LV, JEOL, Japan). The accelerating voltage used was 18 kV.

Determination of functional groups onto the algal biomass by Fourier transform infrared

Fine powdered dried algal samples (raw and element loaded biomasses) were pressed into KBr pellets prior to analysis by FTIR Spectrophotometer (8201 DC, Shimadzu, Japan) (wavenumber range from 400 to 4000 cm^{-1}).

Application of algal biomasses in the treatment of real polluted industrial effluents in Borg El-Arab region

Twenty-one wastewater samples were collected from Borg El-Arab city during March to December 2010. The brown algal biomass *Colpomenia sinuosa* was applied under the concluded optimum conditions from the batch experiments (S/L ratio 1:1000 (*w/v*), contact time: 1 h, temperature: 40 °C). No pH adjustment was done in order to avoid the precipitation of some metals. Heavy metals (Al, Co, Cr, Mo, and V) and trace elements (Fe, Mn, Cu, Ni, and Zn) were determined by inductively coupled argon plasma (iCAP 6500 Duo, Thermo Scientific, England). The removal percentage was calculated using the following equation: Removal (%) = $(C_i\text{-}C_f/C_i) \times 100$, where C_i is the initial element concentration before treatment and C_f is the final element concentration after treatment.

Statistical analysis

All determinations were made in triplicate for all assays. Data were subjected to an analysis of variance (ANOVA) with statistical significance at $P < 0.05$ being tested using the Duncan's test (Waller and Duncan 1969). In the tables means having the same letters in the same column are not significant at P (significance probability value) = 0.05 level.

Results and discussion

Effect of contact time on element biosorption

Data in Table 1 shows that the efficiency of biosorption process increased with increasing of contact time in each case. The biosorption process is very fast during the initial stage, and afterwards, the rate of biosorption process becomes slower near to equilibrium, which is practically obtained after 1 h. The biosorption efficiency remained more or less constant thereafter up to 24 h. Bakatula et al. (2014) stated that biosorption occurred in two steps: the first step corresponds to the dissociation of the complexes formed between metals in solution and water hydronium ions followed by the interaction of metal with algae functional groups.

Effect of pH on element biosorption efficiency

It can be observed from Table 1 that the biosorption efficiency of the three investigated metals increases with increasing pH value. The optimum pH for biosorption of Al^{3+}, Fe^{3+}, and Zn^{2+} are 4, 3, and 6, respectively, in case of the three used algal biomasses.

Both the ionic forms of the metal ions in solution and the electrical charges of the algal cell wall components depend on the solution pH (Aboulsoud 2008). The low degree of biosorption at low pH values can be explained by the fact that at low pH, the H^+ ion concentration is high, and therefore, protons can compete with the metal cations for surface sites (Sarı and Tuzen 2009).

Table 1 Interaction effect between algal type and both of time intervals and aqueous solution pH on metal biosorption efficiency (±SD, $n = 3$) (time experimental conditions: S/L ratio 1/1000 (*w*/*v*), temperature: 25 °C, initial metal concentration: 500 mg L^{-1}, solution pH: 3.1, 2.0, and 4.9 for Al, Fe, and Zn, respectively) (pH experimental conditions: S/L ratio 1/1000 (*w*/*v*), temperature: 25 °C, initial metal concentration: 500 mg L^{-1}, contact time: 1 h)

Algal type	Time	Biosorption (mg g^{-1})			pH	Biosorption (mg g^{-1})		
		Al^{3+}	Fe^{3+}	Zn^{2+}		Al^{3+}	Fe^{3+}	Zn^{2+}
Gelidium latifolium	5 min	7.423 ± 0.04 p	9.19 ± 0.07 p	9.11 ± 0.06 n	1	6.77 ± 0.05 l	19.19 ± 0.06 H	23.04 ± 0.09 p
	10 min	14.14 ± 0.09 m	20.48 ± 0.06 l	26.74 ± 0.02 k	2	23.65 ± 0.06 i	40.62 ± 0.04 F	35.59 ± 0.02 m
	15 min	24.9 ± 0.07 k	26.55 ± 0.03 k	46.31 ± 0.03 h	3	39.96 ± 0.02 f	48.55 ± 0.05 C	43.73 ± 0.05 k
	30 min	29.46 ± 0.05 h	30.28 ± 0.08 j	53.8 ± 0.04 f	4	45.45 ± 0.04 c		50.65 ± 0.06 i
	45 min	34.64 ± 0.03 g	35.19 ± 0.01 h	60.45 ± 0.07 d	5			62.76 ± 0.04 f
	1 h	39.87 ± 0.11 e	40.54 ± 0.02 d	61.61 ± 0.05 d	6			85.01 ± 0.03 c
	2 h	39.46 ± 0.03 ef	39.73 ± 0.03 de	61.68 ± 0.02 d				
	4 h	38.83 ± 0.07 f	39.92 ± 0.06 de	61.75 ± 0.09 d				
	8 h	39.05 ± 0.09 ef	40.05 ± 0.09 de	61.21 ± 0.06 d				
	24 h	39.05 ± 0.13 ef	39.57 ± 0.02 ef	60.62 ± 0.07 d				
Ulva lactuca	5 min	10.33 ± 0.05 o	10.0 ± 0.04 o	12.18 ± 0.08 m	1	19.42 ± 0.02 k	19.66 ± 0.11 Gh	27.12 ± 0.03 o
	10 min	15.72 ± 0.09 l	20.26 ± 0.02 l	26.81 ± 0.04 k	2	29.39 ± 0.05 h	42.52 ± 0.06 E	40.28 ± 0.07 l
	15 min	27.5 ± 0.03 i	29.76 ± 0.05 j	38.99 ± 0.07 i	3	42.56 ± 0.06 e	50.09 ± 0.04 B	48.57 ± 0.09 j
	30 min	34.32 ± 0.07 g	34.76 ± 0.04 h	52.13 ± 0.02 g	4	48.39 ± 0.08 b		55.52 ± 0.01 h
	45 min	39.41 ± 0.08 ef	38.79 ± 0.08 f	61.62 ± 0.01 d	5			67.53 ± 0.04 e
	1 h	42.35 ± 0.06 cd	43.22 ± 0.03 c	67.1 ± 0.08 b	6			89.44 ± 0.06 b
	2 h	42.14 ± 0.05 d	43.14 ± 0.09 c	66.64 ± 0.07 b				
	4 h	42.2 ± 0.03 d	43.24 ± 0.02 c	66.74 ± 0.11 b				
	8 h	41.88 ± 0.06 d	42.95 ± 0.06 c	66.88 ± 0.06 b				
	24 h	41.94 ± 0.15 d	42.95 ± 0.03 c	67.46 ± 0.03 b				
Colpomenia sinuosa	5 min	11.72 ± 0.07 n	11.6 ± 0.11 n	13.62 ± 0.07 m	1	21.12 ± 0.13 j	20.41 ± 0.09 Gh	29.55 ± 0.04 n
	10 min	26.45 ± 0.05 j	18.9 ± 0.05 m	23.11 ± 0.06 l	2	32.3 ± 0.07 g	44.9 ± 0.02 D	43.48 ± 0.07 k
	15 min	34.86 ± 0.07 g	31.26 ± 0.04 i	35.8 ± 0.02 j	3	44.64 ± 0.05 d	53.28 ± 0.07 A	50.95 ± 0.02 i
	30 min	39.41 ± 0.04 ef	37.67 ± 0.08 g	56.22 ± 0.11 e	4	50.94 ± 0.03 a		58.51 ± 0.01 g
	45 min	42.59 ± 0.02 bcd	42.79 ± 0.07 c	64.79 ± 0.10 c	5			70.46 ± 0.08 d
	1 h	43.59 ± 0.06 a	45.32 ± 0.03 a	70.36 ± 0.05 a	6			92.63 ± 0.14 a
	2 h	43.49 ± 0.03 a	44.49 ± 0.13 ab	69.81 ± 0.08 a				
	4 h	43.29 ± 0.04 ab	44.87 ± 0.04 ab	70 ± 0.05 a				
	8 h	43.12 ± 0.02 abc	44.37 ± 0.06 b	70.11 ± 0.03 a				
	24 h	43.1 ± 0.04 abc	44.54 ± 0.04 ab	70.04 ± 0.07 a				

Effect of initial metal concentration on biosorption of metals

As can be seen in Table 2, the metal biosorption efficiency increases with increasing the initial metal concentrations to give the highest removal values at 1000 mg L^{-1} where equilibrium is attained (the optimum concentration).

This attitude may be interpreted by the increase of interaction probability between heavy metals and functional groups from biosorbent surface with increasing of initial concentration of studied metal ions (Bulgariu and Bulgariu 2014). The binding sites at the cell wall of the alga seemed to become saturated with the metal ions at high concentration, which led to a corresponding steadiness in the efficiency of the metal uptake (Elrefaii et al. 2012).

Effect of temperature on metal biosorption

The biosorption of metals is investigated as a function of temperature ranging from 298 to 333 K (25–60 °C). Working above this range of temperature is avoided at high temperatures, the structure of the biomass might be changed and the active sites destroyed (Aboulsoud 2008).

As shown in Table 2, the metal biosorption is slightly increased with rise in temperature from 298 to 333 K showing a slight endothermic nature. In general, the formation of

Table 2 Interaction effect between algal type and both of initial metal concentration and temperature on biosorption efficiency (±SD, $n = 3$) (concentration experimental conditions: S/L ratio 1/1000 (w/v), temperature: 25 °C, contact time: 1 h, solution pH: 4, 3, and 6 for Al^{3+}, Fe^{3+}, and Zn^{2+}, respectively) (temperature experimental conditions: S/L ratio 1/1000 (w/v), initial metal concentration: 1000 mg L^{-1}, contact time: 1 h, solution pH: 4, 3, and 6 for Al^{3+}, Fe^{3+}, and Zn^{2+}, respectively)

Algal type	Metal Conc. (mg L^{-1})	Biosorption (mg g^{-1})			Temp. (°C)	Biosorption (mg g^{-1})		
		Al^{3+}	Fe^{3+}	Zn^{2+}		Al^{3+}	Fe^{3+}	Zn^{2+}
Gelidium latifolium	0.5	0.436 ± 0.08 p	0.423 ± 0.07 r	0.467 ± 0.09 s	25	56.79 ± 0.05 f	61.09 ± 0.07 F	101.3 ± 0.16 f
	1	0.908 ± 0.06 p	0.915 ± 0.08 q	0.922 ± 0.13 r	40	57.84 ± 0.03 e	61.96 ± 0.05 e	102.2 ± 0.09 e
	5	4.017 ± 0.01 o	3.856 ± 0.03 p	4.092 ± 0.04 q	60	58.29 ± 0.08 e	62.68 ± 0.01 d	102.3 ± 0.08 e
	10	5.954 ± 0.05 n	8.147 ± 0.09 o	8.514 ± 0.06 p				
	25	22.56 ± 0.02 m	21.07 ± 0.04 n	22.63 ± 0.09 o				
	50	35.16 ± 0.11 l	37.88 ± 0.03 m	43.49 ± 0.05 n				
	100	37.02 ± 0.13 j	42.66 ± 0.02 k	48.94 ± 0.11 l				
	250	40.17 ± 0.09 h	43.52 ± 0.11 j	79 ± 0.06 i				
	500	45.46 ± 0.05 g	48.56 ± 0.07 g	85.01 ± 0.03 g				
	1000	56.79 ± 0.11 c	61.09 ± 0.03 c	101.29 ± 0.02 c				
Ulva lactuca	0.5	0.437 ± 0.03 p	0.424 ± 0.08 r	0.468 ± 0.05 s	25	60.89 ± 0.07 d	62.52 ± 0.06 de	107.3 ± 0.07 d
	1	0.911 ± 0.02 p	0.918 ± 0.04 q	0.924 ± 0.04 r	40	61.71 ± 0.06 c	62.71 ± 0.02 d	108.3 ± 0.04 c
	5	4.03 ± 0.06 o	3.867 ± 0.05 p	4.101 ± 0.03 q	60	62.02 ± 0.02 c	63.04 ± 0.05 d	108.5 ± 0.01 c
	10	5.974 ± 0.04 n	8.171 ± 0.06 o	8.534 ± 0.07 p				
	25	22.67 ± 0.09 m	21.16 ± 0.02 n	22.69 ± 0.01 o				
	50	35.45 ± 0.08 kl	38.13 ± 0.03 m	43.65 ± 0.08 mn				
	100	38.46 ± 0.02 i	43.89 ± 0.05 i	50.08 ± 0.04 k				
	250	45.06 ± 0.11 g	48.33 ± 0.08 g	82.97 ± 0.03 h				
	500	48.39 ± 0.14 e	50.1 ± 0.09 f	89.44 ± 0.05 e				
	1000	60.89 ± 0.07 b	62.52 ± 0.11 b	107.29 ± 0.07 b				
Colpomenia sinuosaz	0.5	0.439 ± 0.07 p	0.426 ± 0.07 r	0.469 ± 0.08 S	25	62.93 ± 0.08 b	65.15 ± 0.09 c	110.3 ± 0.07 b
	1	0.915 ± 0.09 o	0.921 ± 0.03 q	0.927 ± 0.06 R	40	63.79 ± 0.03 a	65.95 ± 0.02 b	111.6 ± 0.05 a
	5	4.049 ± 0.03 o	3.883 ± 0.07 p	4.114 ± 0.05 Q	60	63.97 ± 0.07 a	66.56 ± 0.04 a	111.7 ± 0.04 a
	10	6.004 ± 0.05 n	8.206 ± 0.02 o	8.563 ± 0.03 P				
	25	22.84 ± 0.01 m	21.29 ± 0.05 n	22.78 ± 0.04 O				
	50	35.87 ± 0.07 kl	38.51 ± 0.08 l	43.88 ± 0.02 mn				
	100	40.59 ± 0.11 h	45.73 ± 0.09 h	51.78 ± 0.07 J				
	250	47.33 ± 0.09 f	50.5 ± 0.03 e	88.87 ± 0.04 F				
	500	50.94 ± 0.08 d	53.28 ± 0.05 d	92.63 ± 0.03 d				
	1000	62.93 ± 0.06 a	65.15 ± 0.02 a	110.29 ± 0.15 a				

coordination complexes between transition metal cations and carboxylate ligands is endothermic (Vilar et al. 2005). Although there is no significant difference between biosorption efficiency at 40° and 60 °C, 40 °C was chosen as the optimum temperature for metal biosorption as it is as similar as possible to the Egyptian climatic conditions.

Thermodynamic studies

Figure 1 shows the Van't Hoff plots of $ln\ K_c$ versus $1/T$, and Table 3 shows the thermodynamic parameters that are calculated from the slopes and intercepts of the straight lines.

The positive values of (ΔG) indicated the nonspontaneous nature of adsorption for the three tested metals using all algal biomasses (Aksu 2002). The positive values of (ΔH) show the endothermic nature of the biosorption, which is an indication of the existence of a strong interaction between algal biomasses and the three metals under study. The positive enthalpy of adsorption obtained indicates chemical adsorption. This suggests that the chemical bonds between the algal surface and the metal molecules are strong enough and the metal molecules cannot be easily desorbed by physical means such as simple shaking or heating (Farah and El-Gendy 2013). The negative values of (ΔS) show the decreased randomness at the

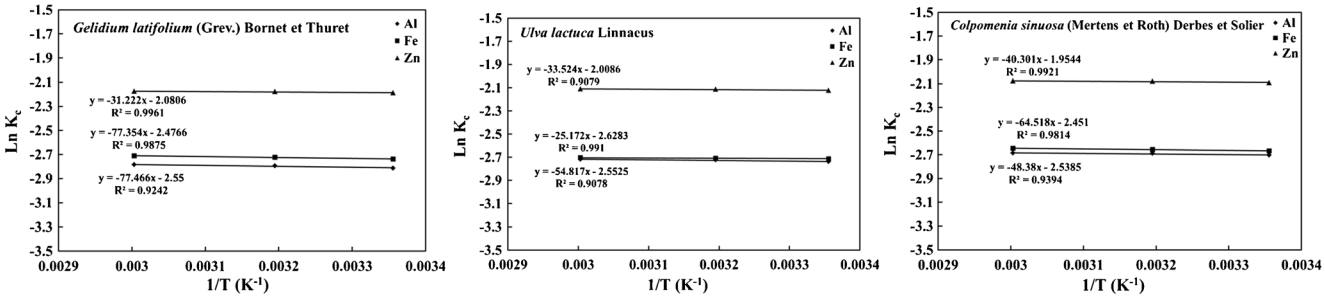

Fig. 1 Van't Hoff plot of ln K_c versus 1/T for heavy metal biosorption

solid/solution interface during the biosorption of the metals on algal biomass, reflecting that the metal molecules were orderly adsorbed on the surface of the algal biomasses (Saibaba and King 2013).

Table 3 Thermodynamic parameters and equilibrium parameters of Langmuir and Freundlich models for metal biosorption

Heavy metal	Temperature (K)	Thermodynamic parameters				Langmuir parameters			Freundlich parameters			$q_{e\ (exp)}$ (mg g^{-1})
		ΔG (J mol^{-1})	ΔS (J mol^{-1} K^{-1})	ΔH (298–333) (J mol^{-1})	R^2	K_L (L mg^{-1})	Q_e (mg g^{-1})	R^2	K_F	*n*	R^2	
Gelidium latifolium												
Al^{3+}	298	8256.09	−25.54	644.05	0.924	0.139	55.6	0.999	5.51	1.21	0.989	56.78
	313	8556.26	−25.27									
	333	8997.74	−25.08									
Fe^{3+}	298	8067.83	−24.91	643.12	0.987	0.135	63.3	0.995	6.26	1.17	0.988	61.08
	313	8369.68	−24.68									
	333	8788.35	−24.46									
Zn^{2+}	298	5937.88	−19.05	259.58	0.996	0.107	103.1	0.994	8.9	1.1	0.996	101.29
	313	6184.64	−18.9									
	333	6543.04	−18.86									
Ulva lactuca												
Al^{3+}	298	7696	−24.29	455.74	0.907	0.14	56.2	0.9998	5.64	1.21	0.989	60.89
	313	8000.27	−24.1									
	333	8438.44	−23.97									
Fe^{3+}	298	7138.92	−23.25	209.28	0.991	0.136	64.1	0.9957	6.42	1.17	0.988	62.52
	313	7468.61	−23.19									
	333	7903.76	−23.1									
Zn^{2+}	298	5817.06	−18.58	278.71	0.907	0.109	104.2	0.9941	9.12	1.1	0.996	107.29
	313	6054.4	−18.45									
	333	6401.26	−18.38									
Colpomenia sinuosa												
Al^{3+}	298	7501.8	−23.82	402.23	0.939	0.144	57.1	0.999	5.84	1.2	0.99	62.93
	313	7801.35	−23.63									
	333	8240.11	−23.53									
Fe^{3+}	298	7684.28	−23.98	536.4	0.981	0.14	64.9	0.995	6.64	1.17	0.989	65.15
	313	7982.81	−23.79									
	333	8397.35	−23.6									
Zn^{2+}	298	5853.12	−18.51	335.06	0.992	0.112	105.3	0.993	9.44	1.1	0.996	110.29
	313	6080.25	−18.35									
	333	6421.48	−18.27									

Summarizing these results, the biosorption mechanism of the three studied metals is nonspontaneous, endothermic, chemical, and orderly adsorption on the surface of the algal surface.

Biosorption isotherm modeling

As can be observed from Table 3 and Figs. 2 and 3, the calculated (Q_e) values match with the experimental ones ($q_{e\ (exp)}$) that are determined in the level of high concentrations. These results reflect the applicability of biosorption in the treatment of water samples that contain low and high concentrations of metals. On the other hand, K_L values indicate the adsorption affinity of the binding sites where the good sorption is indicated by low values of Langmuir parameter (Kumar et al. 2005). This assumption is confirmed as the higher (K_L) calculated values are found to be inversely proportional to the actual high biosorption capacities ($q_{e\ (exp)}$) and vice versa.

The values of Freundlich constant (n) that are greater than unity indicate the favorability of the algal biomass to biosorb metals from water. Also, the higher adsorption capacity (K_F) indicates the strong electrostatic attraction force (Kumar et al. 2005); therefore, the higher (K_F) calculated values are found to be proportional to the actual high biosorption capacities ($q_{e\ (exp)}$) and vice versa.

The best-fit equilibrium model was determined based on the linear regression correlation coefficient (R^2). It can be reported that Freundlich isotherm model fitted slightly better than the Langmuir model in case of divalent Zn biosorption; meanwhile, Langmuir model fitted better in case of trivalent Al and Fe. This finding indicates that probably the sorption of Zn^{2+} was a multilayer coverage (heterogeneous sorption); meanwhile, the sorption of Al^{3+} and Fe^{3+} was monolayer coverage (homogeneous sorption). This finding agrees with Sarı and Tuzen (2009) and Bakatula et al. (2014) where they reported the best fitting of Langmuir model in case of Al^{3+} and Fe^{3+} biosorption using the brown alga *Padina pavonica* and the green alga *Oedogonium* sp., respectively. On the other hand, Liu et al. (2009) reported the best fitting of Freundlich model in case of Zn biosorption using the brown alga *Saccharina (Laminaria) japonica*.

The three algal biomass affinity to heavy metal biosorption follows the same sequence of $Zn^{2+} > Fe^{3+} > Al^{3+}$. This affinity order may be attributed to the more or less decrease of ionic radii in the same sequence: 0.75, 0.55, and 0.53 Å, respectively (Wells 1975). As a general rule, there is a preferential binding of heavier ions to active sites which can be due to stereochemical effects; larger ions might better fit a binding site with two distinct active groups (Figueira et al. 2000). Another explanation may be conducted on the light of the equilibrium isotherm results in the current study that reveals the multilayer coverage of Zn^{2+} versus the monolayer coverage of Al^{3+} and Fe^{3+} that leads to higher Zn^{2+} biosorption.

Reusability and regeneration of algal biomasses

High numbers of cycles of biosorption-desorption-resorption that the biosorbent can achieve are desirable to make the process more economical. The reuse of the biomass and desorbent is an important feature for its possible utilization in continuous systems in industrial processes (Deng et al. 2006).

Figure 4 shows the desorption efficiency using 0.01 M Na_2EDTA for four reuse cycles of sorption-desorption. After one reuse cycle, the desorption % in case of *G. latifolium* reaches 91.33, 91.94, and 93.89% for Al^{3+}, Fe^{3+}, and Zn^{2+}, respectively. The desorption % in case of *U. lactuca* reaches 91.17, 92.02, and 91.66% for Al^{3+}, Fe^{3+}, and Zn^{2+}, respectively. The desorption % in case of *C. sinuosa* reaches 90.65, 90.58, and 90.64% for Al^{3+}, Fe^{3+}, and Zn^{2+}, respectively. Similar results were obtained by Deng et al. (2006) where 0.01 M Na_2EDTA recovered 94.7% of Cu^{2+} and 82.5% of Pb^{2+} bound to the green biomass *Cladophora fascicularis* but within 18 h.

The desorption efficiency decreases with increasing cycle number, as after four reuse cycles reach 62.15, 68.37, and 68.2% for Al^{3+}, Fe^{3+}, and Zn^{2+}, respectively, in case of *G. latifolium*, while the desorption % in case of *U. lactuca* reaches 65.34, 70.01, and 67.1% for Al^{3+}, Fe^{3+}, and Zn^{2+}, respectively. The desorption % in case of *C. sinuosa* reaches 65.29, 65.82, and 66.53% for Al^{3+}, Fe^{3+}, and Zn^{2+}, respectively.

Figure 5 shows the resorption efficiency of Al^{3+}, Fe^{3+}, and Zn^{2+} for four reuse cycles of desorption-resorption. After one reuse cycle, the highest resorption % reaches 77.4, 76.88, and 77.17% in case of *C. sinuosa* for Al^{3+}, Fe^{3+}, and Zn^{2+}, respectively. Then, the middle resorption % reaches 76.09, 75.7, and 76.59% in case of *U. lactuca* for Al^{3+}, Fe^{3+}, and Zn^{2+}, respectively. The lowest resorption % reaches 73.96, 75.04, and 75.07% in case of *G. latifolium* for Al^{3+}, Fe^{3+}, and Zn^{2+}, respectively.

The resorption efficiency decreases with increasing cycle number, as after four reuse cycles, the highest resorption % reaches 51.28, 51.63, and 53.28% for Al^{3+}, Fe^{3+}, and Zn^{2+}, respectively, using *C. sinuosa*. Then, the middle resorption % reaches 49.09, 49.14, and 51.98% in case of *U. lactuca* for Al^{3+}, Fe^{3+}, and Zn^{2+}, respectively. The lowest resorption % reaches 45.16, 48.16, and 48.98% in case of *G. latifolium* for Al^{3+}, Fe^{3+}, and Zn^{2+}, respectively. Similar results were obtained by Aboulsoud (2008) who stated that resorption % after five reuse cycles reached 45.28% using Na_2EDTA.

As can be seen, both of desorption and resorption efficiencies decrease with increasing the reusability cycle number. A possible cause of reduction in the biosorption capacity of algal biomass can be attributed to the adverse effect of the eluent on the binding sites of the algal cell wall components (Tüzün

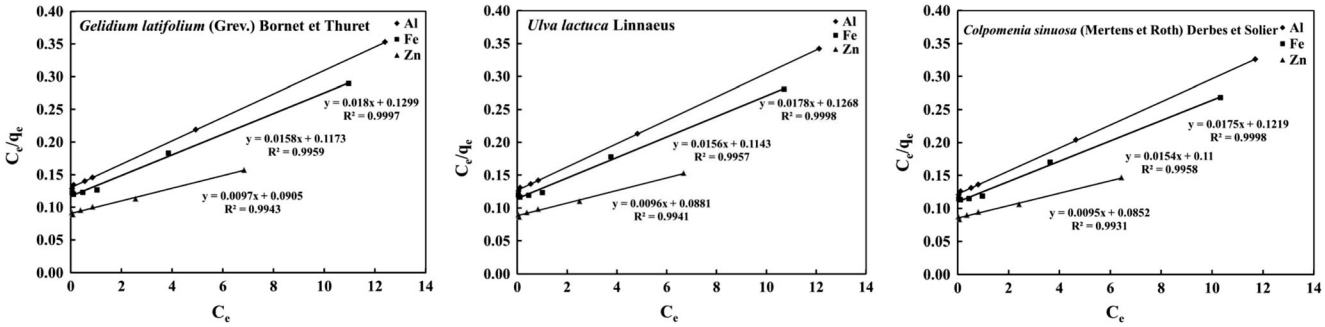

Fig. 2 Linearized Langmuir adsorption isotherms for metal biosorption

et al. 2005). Also, accumulation of remaining metal molecules inside the algal biomass in each cycle acts to decrease the further resorption efficiency in the next cycle. The algal biomasses can be reused up to four cycles with a reasonable efficiency in all cases.

Examination of algal biomass surface using scanning electron microscope

The SEM micrographs of the biosorbent material before and after metal biosorption are illustrated in Fig. 6. By comparing with the surface of the raw biomasses between algal biomasses, it is clear that each algal type shows a unique surface structure. The surface of the red alga *G. latifolium* appears smooth and non-porous, the green alga *U. lactuca* poses a papillary surface structure supplying a large exposed surface area for biosorption; meanwhile, the brown algal biomass *C. sinuosa* surface is stratified in shape and extensively papillary providing a larger exposed surface area for biosorption.

It is obviously seen that the morphological changes in the cell wall surface due to metal biosorption. The red algal biomass *G. latifolium* is ruptured due to loading with Al^{3+}; meanwhile, little cavities appeared due to Fe^{2+} loading and the surface appeared wrinkled in case of Zn^{2+} loading. The green algal biomass *U. lactuca* shows a surface protuberance in case of Al^{3+} loading; also, Fe^{2+}-loaded biomasses have a plump shape surface; meanwhile, Zn^{2+} loading shows a more protuberance accompanied with wrinkling of surface. The brown algal biomass *C. sinuosa* surface becomes rough due to Al^{3+} loading while preserving of the stratified structure; oppositely, the stratified algal surface changes and shows large cavities due to the Fe^{2+} loading and becomes ruptured due to Zn^{2+} loading.

The morphology change according to Tamilselvan et al. (2013) might be due to the binding of metals in the surface of the biomass. Moreover, this change is probably caused due to strong cross-linking due to the chemisorption (concluded from thermodynamic studies) between the metals' molecules and the active groups in the cell wall matrix.

Similar results were obtained by Arief et al. (2008), Natarajan et al. (2011), and Shukla and Shukla (2013).

Fourier transform infrared analysis of algal biomasses

Table 4 shows the FTIR spectra of raw algal biomasses and loaded ones by metals under investigation. The FTIR spectra are in the range of 400–4000 cm^{-1}. It exhibits absorption bands indicating the presence of C–N–S, alcoholic C–O, S=O, carboxylic C–O, carboxylic C=O, NH, and OH groups. The frequencies of functional groups can be firmly discussed as follows:

- C–N–S group:

The spectra of C–N–S display transmittance band at 474, 470, and 532 cm^{-1} in case of the red algal biomass

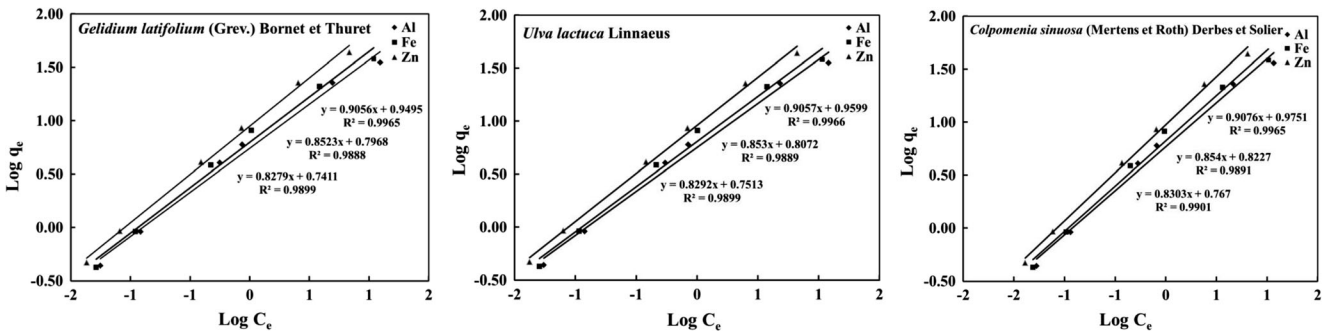

Fig. 3 Linearized Freundlich adsorption isotherms for metal biosorption

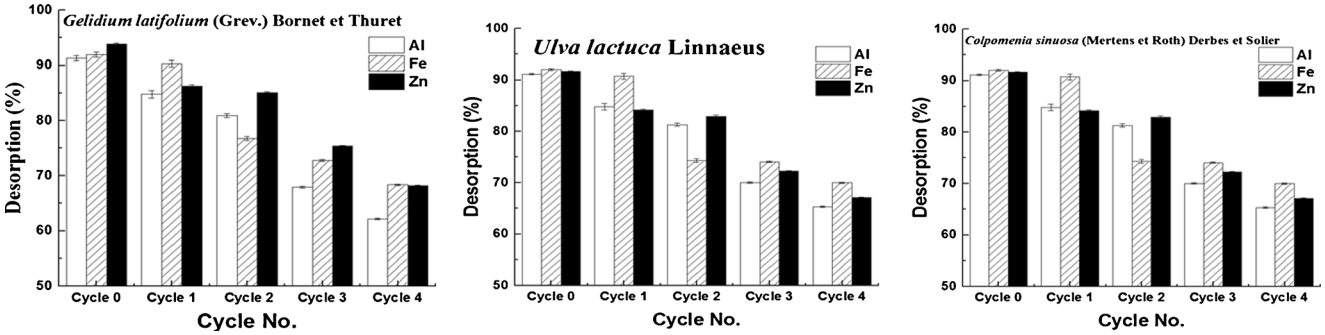

Fig. 4 Effect of reuse cycles on desorption efficiency of heavy metals and trace elements (±SD, $n = 3$) (experimental conditions: eluent concentration: 0.01 M Na_2EDTA, S/L ratio of 1/250 (*w*/*v*), temperature: 25 °C, contact time: 2 h)

G. latifolium, the green algal biomass *U. lactuca*, and the brown algal biomass *C. sinuosa*, respectively. After metal biosorption, these bands are shifted to wavenumbers ranging from 459 to 597 cm^{-1} indicating the participation of C–N–S group in Al^{3+}, Fe^{3+}, and Zn^{2+} biosorption process especially in case of the brown algal biomass where the band shift is acute and more obvious. Bulgariu and Bulgariu (2014) in their study on *U. lactuca* stated the thiocyanate (C–N–S) shearing due to polypeptide structure of algae cells at 574–464 cm^{-1}.

- C–O of alcoholic group:

The spectra of C–O of alcoholic group display transmittance band at 1114 cm^{-1} for the three algal biomasses. Only in *G. latifolium*, these bands are shifted after metal biosorption to lower wavenumbers is ranged from 1072 to 1076 cm^{-1} indicating the participation of C–O of alcoholic group in Al^{3+}, Fe^{3+}, and Zn^{2+} biosorption process. Meanwhile, no band shift is observed in case of green and brown algal biomasses in case of all metals under study revealing that C–O of alcoholic group is not participated in such cases. Bulgariu and Bulgariu (2014) in their study on *U. lactuca* also reported C–OH band at 1031 cm^{-1}.

- S=O of sulfonate group:

The spectra of S=O of sulfonate group display transmittance band at 1284, 1280, and 1280 cm^{-1} in *G. latifolium*, *U. lactuca*, and *C. sinuosa*, respectively. Only in case of Fe^{3+} biosorption by the three algal biomasses, these bands are shifted to lower wavenumbers ranging from 1261 to 1203 cm^{-1} indicating the participation of S=O of sulfonate group in Fe^{3+} biosorption process. The band shift is acute and more obvious in *C. sinuosa*. No shifting is observed after $Al^{3+}$and Zn^{2+} biosorption reflecting that this group is not contributed in their biosorption by the three algal biomasses. It is worth to mention that Figueira et al. (1999) reported the contribution of sulfonate group in removal of Fe^{3+} by the brown algal biomass *Sargassum fluitans*. Fakhry (2013) observed absorbance band at 1200 cm^{-1} corresponding to the sulfonate ($–OSO_3$) group in the alga *Padina pavonica*.

- Carboxylic C–O:

The spectra of C–O of carboxylic group display transmittance band at 1411, 1404, and 1411 cm^{-1} in *G. latifolium*, *U. lactuca*, and *C. sinuosa*, respectively. After Al^{3+}, Fe^{3+}, and Zn^{2+} biosorption, these bands are shifted to lower wavenumber of 1384 cm^{-1} for all algal biomasses indicating the participation of C–O of carboxylic group in Al^{3+}, Fe^{3+}, and Zn^{2+} biosorption process. Aboulsoud (2008)

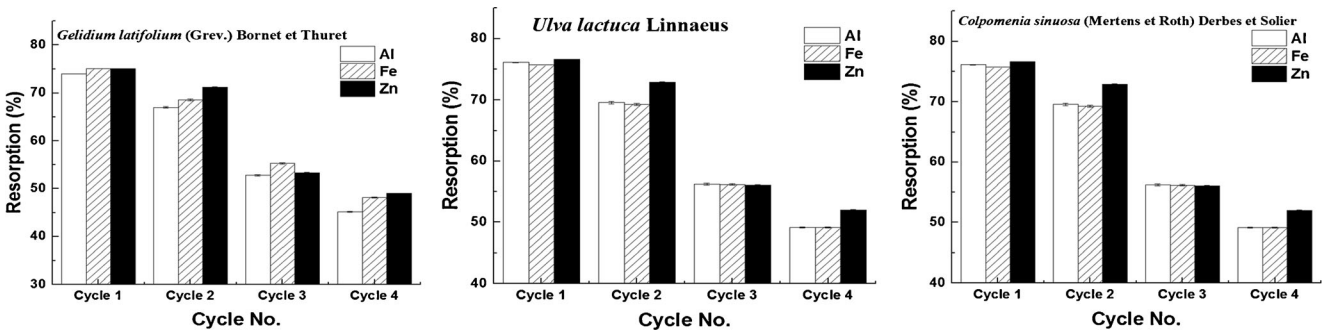

Fig. 5 Effect of reuse cycles on resorption efficiency of heavy metals and trace elements (±SD, $n = 3$) (experimental conditions: S/L ratio: 1/1000 (*w*/*v*), temperature: 40 °C, contact time: 1 h, initial metal concentration: 1000 mg L^{-1}, solutions' pH: 4, 3, and 6 for Al^{3+}, Fe^{3+}, and Zn^{2+}, respectively)

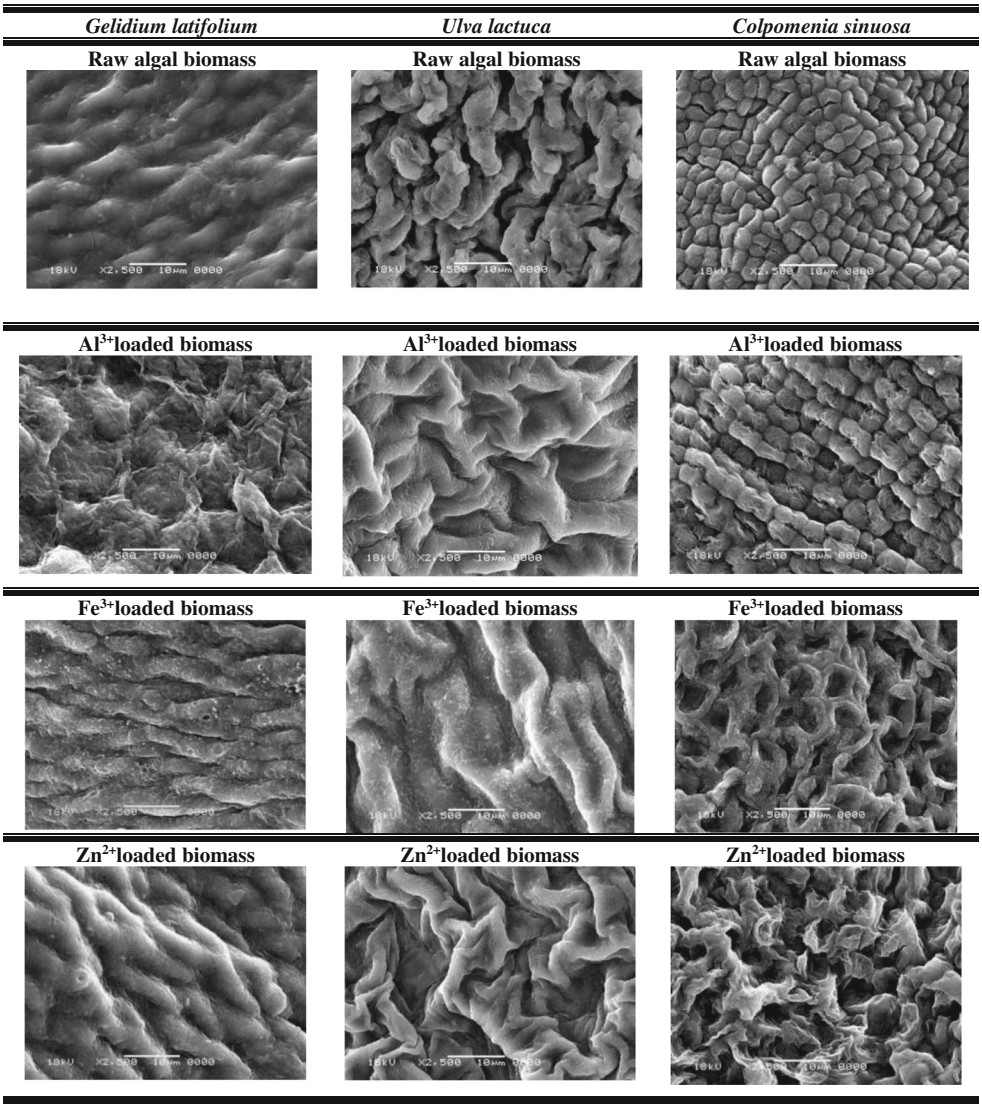

Fig. 6 The SEM micrographs of the algal biomasses before and after metal biosorption at ×2500 magnification

observed absorbance band at 1411 cm^{-1} corresponding to the C–O of carboxylic group in biomass of *Sargassum hornschuchii*.

- Carboxylic C=O:

The spectra of C=O of carboxylic group display transmittance band at 1635, 1631, and 1631 cm^{-1} in *G. latifolium*, *U. lactuca*, and *C. sinuosa*, respectively. After Al^{3+}, Fe^{3+}, and Zn^{2+} biosorption by the three algal biomasses, these bands are shifted to higher wavenumbers that are ranged from 1627 to 1639 cm^{-1} indicating the participation of C=O of carboxylic group in Al^{3+}, Fe^{3+}, and Zn^{2+} biosorption process. This finding agrees with the thermodynamic studies in the present study where the biosorption process was proven to be endothermic in nature, as Vilar et al. (2005) stated that the formation of coordination complexes between transition metal cations and carboxylate ligands is endothermic. Fakhry (2013) observed absorbance band at 1670 cm^{-1} corresponding to the C=O of carboxylic group in the alga *Padina pavonica*.

- NH group:

The spectra of NH group display transmittance band at 3417, 3414, and 3444 cm^{-1} in *G. latifolium*, *U. lactuca*, and *C. sinuosa*, respectively. After $Al^{3+}$and Zn^{2+} biosorption by the three algal biomasses, these bands are shifted to wavenumber of 3421 cm^{-1} indicating the participation of NH group in Al^{3+} and Zn^{2+} biosorption process. Meanwhile, no shift is observed in case of Fe^{3+} biosorption reflecting that this group is not contributed in its biosorption by the three algal biomasses. Fakhry (2013) observed absorbance band at 3400 cm^{-1} corresponding to the NH group in *P. pavonica*.

Table 4 FTIR frequencies for algal biomasses before and after metal biosorption

Algal form	Wavenumber (cm^{-1})						
	C–N–S	C–O alcoholic	S=O	Carboxylic group		NH	OH
				C–O	C=O		
Gelidium latifolium							
Raw	474	1114	1284	1411	1635	3417	3645
Al^{3+} loaded	459	1076	1280	1384	1637	3421	3971
Fe^{3+} loaded	462	1076	1253	1384	1639	3417	3969
Zn^{2+} loaded	472	1072	1280	1384	1639	3421	3973
Ulva lactuca							
Raw	470	1114	1280	1404	1631	3414	3749
Al^{3+} loaded	459	1114	1280	1384	1627	3421	3749
Fe^{3+} loaded	478	1114	1261	1384	1627	3414	3749
Zn^{2+} loaded	474	1114	1280	1384	1627	3421	3749
Colpomenia sinuosa							
Raw	532	1114	1280	1411	1631	3444	3749
Al^{3+} loaded	578	1114	1280	1384	1635	3421	3961
Fe^{3+} loaded	597	1114	1203	1384	1635	3444	3961
Zn^{2+} loaded	567	1114	1280	1384	1635	3421	3946

- OH group:

The spectra of OH group display transmittance band at 3645, 3749, and 3749 cm^{-1} in *G. latifolium*, *U. lactuca*, and *C. sinuosa*, respectively. After Al^{3+}, Fe^{3+}, and Zn^{2+} biosorption, these bands are shifted to wavenumbers that are ranged from 3946 to 3973 cm^{-1} in case of *G. latifolium* and *C. sinuosa* indicating the participation of OH group in Al^{3+}, Fe^{3+}, and Zn^{2+} biosorption process. No band shift is observed in case of Al^{3+}, Fe^{3+}, and Zn^{2+} biosorption by *U. lactuca* reflecting that this group does not contribute metal biosorption by this algal type. Jones (2000) reported the absorbance band of OH group at 3600–3700 cm^{-1}.

Application of biosorption optimum conditions in the treatment of real polluted industrial wastewater samples from Borg El-Arab region

The batch experiment results show that the brown algal biomass is an effective and economical biosorbent material for the removal and recovery of heavy metal ions. The highest biosorption efficiency reached 63.78, 65.95, and 111.57 mg g^{-1} for Al^{3+}, Fe^{3+}, and Zn^{2+}, respectively, using *C. sinuosa* under the optimum biosorption conditions (initial element concentration, 1000 mg L^{-1}; temperature, 40 °C; contact time, 1 h; pH, 4, 3, and 6 for Al3+, Fe3+, and Zn2+, respectively); thus, it is applied in removal of heavy metals and trace elements from 21 industrial wastewater samples under the optimum concluded conditions. The quality of wastewater samples was assessed according to the Egyptian Law No. 4 of 1994 promulgating the environment Law and its amendments in Law No. 9 of 2009. Only the violating concentrations are focused in the following discussion.

In the textile dyeing sector, the violating concentrations reached 14.11, 26.84, and 1.35 mg L^{-1} for Zn, Fe, and Mn, respectively, regarding to the guidelines of 5, 1.5, and 1.00 mg L^{-1}, respectively. These concentrations were lowered to reach 1.87, 1.25, and 0.438 mg L^{-1} by removal percentage of 86.68, 95.33, and 67.6%, respectively. These violating concentrations of Fe and Mn may result from the "metallization" process during the textile dyeing using azodyes (Straley and Fisher 1959). On the other hand, most used dyes contain Zn or other metal atoms in their composition; thus, Zn concentration in dyeing wastewater (acid dyes on wool) reaches 3.4 mg L^{-1} as mentioned by Bisschops and Spanjers (2003); therefore, the high result of Zn concentration probably originated from the dye residues in wastewater.

In the food production sector, the violating concentrations reached 39.03, 84.11, and 83.58 mg L^{-1} for Al, Fe, and Mn, respectively (biscuits production factory). This is regarding to the Egyptian guidelines of 3, 1.5, and 1.00 mg L^{-1} for Al, Fe, and Mn, respectively. These concentrations were lowered to reach 12.67, 9.38, and 4.391 mg L^{-1} by removal percentage of 67.54, 88.84, and 94.75%, respectively. It is noticed that food industrial wastewater is the most polluted

effluent among the factories under study. High Al concentration is mostly due to the residue of baking powder (containing the additive sodium aluminum phosphate) that was reported to contain 2.3 g Al $(100\ g)^{-1}$ (Orme and Ohanian 1990). On the other hand, Fe is extremely in high concentration which is probably due to the "fortification" process of some food staff with iron as it is regularly added to food in many countries to prevent iron deficiency anemia. For example, Fe concentration in different biscuits reaches 15.96 mg $(100\ g)^{-1}$ as reported by Doner and Ege (2004). Meanwhile, Mn is one of the essential minerals and a main component of plenty of food staff. For example, Mn concentration reaches 2.79 mg $(100\ g)^{-1}$ in tea biscuits (Vitali et al. 2008).

In the oil production sector, only Fe concentration reached 2.436 mg L^{-1} and was violating the guidelines of 1.5 mg L^{-1}. This concentration was lowered to be 0.671 mg L^{-1} (72.45 removal %). For many years, Fe is used in the form of $FeCl_3$ as coagulant in demulsifying oily wastes (Abo-El Ela and Nawar 1980).

In the paper and carton production sector, the violating concentrations reached 3.135, 2.818, and 0.6241 mg L^{-1} for Al, Fe, and Ni, respectively. This is in regard to the guidelines of 3, 1.5, and 0.10 mg L^{-1} for Al, Fe, and Ni, respectively. Their concentrations were lowered to reach 0.964, 0.873, and 0.072 mg L^{-1} by removal percentage of 69.25, 68.8, and 88.42%, respectively. As manufacturing of paper is actually a proprietary activity which is strictly protected by each manufacturer, it is difficult to say where certain elements come from, taking into account that the used additives are not of high chemical purity, so it is possible that some elements are introduced as impurities. It is worth to mention that Fe and Ni are main components in paper composition as their concentrations reach 753.4 and 55 mg kg^{-1}, respectively (Rozic et al. 2005).

In the spinning and textile production sector, only Mn concentration was violating the guidelines reaching 3.833 mg L^{-1} regarding to 1.00 mg L^{-1} as guideline concentration. Its concentration was lowered to reach 0.056 mg L^{-1} by 98.54 removal %. This concentration of Mn may result from the metallization process during textile dyeing (Straley and Fisher 1959).

In the soap production sector, four elements, Al, Fe, Mn, and Zn, were exceeding the guidelines as their concentrations reached 9.09, 31.93, 3.76, and 23.67 mg L^{-1}, respectively, with regard to the guidelines of 3, 1.5, 1.00, and 5 mg L^{-1}, respectively. Their concentrations were lowered to reach 3.21, 2.35, 0.87, and 3.21 mg L^{-1} by removal percentage of 64.6, 92.63, 76.84, and 86.42%, respectively. Al and Fe may result from alum and $FeCl_3$ that are used in demulsifying oily wastes (Abo-El Ela and Nawar 1980), whereas Mn was reported to be a constituent of soap composition and was found in soap effluent by 0.351 mg L^{-1} (Faremi and Oloyede 2010). Also, Zn is involved in the composition of soap in the form of zinc pyrithione and zinc carbonate as antimicrobial agent and discoloration inhibitor, respectively (Smith et al. 2012).

In the metals, steel, and concrete production sector, the violating concentrations reached 21.37, 4.388, and 5.01 mg L^{-1} for Mn, Al, and Fe, respectively. This is regarding to the guidelines of 1, 3, and 1.5 mg L^{-1}, respectively. Their concentrations were lowered to reach 0.45, 0.93, and 0.87 mg L^{-1} by removal percentage of 97.86, 78.67, and 82.5%, respectively. The cooling water resulted during steel manufacturing was reported to be polluted with different metals such as Mn (Strugariu and Heput 2012).

In the wood production sector, Fe and Zn concentrations in sample reached 7.743 and 26.22 mg L^{-1} comparing with the Egyptian guidelines of 1.5 and 5 mg L^{-1}, respectively. Their concentrations were lowered to reach 1.471 and 2.65 mg L^{-1} by removal percentage of 81.00 and 89.89%, respectively. Fe may release in wastewater as a result of cellular degradation of wood, where the brown rot fungi produce extracellular H_2O_2 reacts with Fe from wood itself leading to production of Fenton's reagent "$Fe^{++} + H_2O_2$" (Xu and Goodell 2001). On the other hand, many Zn compounds are used as wood preservatives (Goettsche and Reuther 1993).

In the car filter production sector, Cr, Fe, and Zn concentrations were violating the guidelines of 1.00, 1.5, and 5 mg L^{-1} where they reached 10.87, 5.606, and 34.96 mg L^{-1}, respectively. These concentrations were lowered to reach 0.89, 1.33, and 4.78 mg L^{-1} by removal percentage of 91.79, 76.24, and 86.32%, respectively. These three contaminants are among the main components in this industrial sector (Kulekci 2008; Abdullah 2010 and WQA 2013).

In the cosmetics production sector, only Fe concentration is violating the guidelines of 1.5 mg L^{-1} where it reached 3.372 mg L^{-1}. This concentration was lowered to be 0.82 mg L^{-1} (75.65 removal %). The source of Fe may be the iron oxide that used in skin cosmetics as dispersible agent (Yoshio and Tadashi 1995).

In the pharmaceutical production sector, only Zn concentration is greater than the guidelines of 5 mg L^{-1} where it reached 8.144 mg L^{-1}. This concentration was lowered to be 1.38 mg L^{-1} (83.06 removal %). Zn is a component of multivitamin drugs and reported to reach 2.9 mg L^{-1} in wastewater of pharmaceutical industry (Tisler and Koncan 1999).

Borg El-Arab city includes 9 residential areas and 4 industrial zones. All the domestic sewage as well as the industrial wastewater is primary treated at an oxidation pond treatment station (Hussein et al. 2005). Concentrations of Al, Fe, and Zn in the collective industrial wastewater reached 11.29, 8.076, and 17.29 mg L^{-1} comparing with the Egyptian guidelines of 3, 1.5, and 5 mg L^{-1}, respectively. These concentrations were lowered to reach 2.167, 1.14, and 4.37 mg L^{-1} by removal percentage of 80.81, 85.85, and 74.72%, respectively. On the

other hand, concentrations of Al and Fe in the oxidation pond reached 6.156 and 7.894 mg L^{-1}, respectively. Their concentrations were lowered to reach 1.23 and 1.34 mg L^{-1} by removal percentage of 80 and 83%, respectively.

It was achieved that all the violating concentrations of heavy metals are lowered to be less than the guidelines except of Al and Fe in soap production factory that are lowered from 9.091 to 3.218 mg L^{-1} (by 64.6 removal %) and from 31.93 to 2.354 mg L^{-1} (by 92.63 removal %), respectively; and Al, Fe and Mn in food production factory that are lowered from 39.03 to 12.67 mg L^{-1} (by 67.54 removal %), from 84.11 to 9.387 mg L^{-1} (by 88.84 removal %) and from 83.58 to 4.391 mg L^{-1} (by 94.75 removal %), respectively. However, the violating concentrations are lowered to a great extent, but the incomplete removal of heavy metals in these two samples may be attributed to the very high concentrations of the violating metals that are accompanied with low pH values (3.3 and 3.8 for sample Nos. 18 and 20, respectively), where H^+ competes with heavy metal ions for the algal biomass active sites.

In general, the removal efficiency for the determined elements reached 80.81, 38.25, 91.79, 59.96, 95.33, 98.54, 27.39, 88.42, 36.59, and 96.98% for Al, Co, Cr, Cu, Fe, Mn, Mo, Ni, V, and Zn, respectively, through all studied samples.

Conclusions

The studied algal biomasses are natural, low-cost, reusable, and eco-friendly tool showing promising results in the field of water treatment and removal of heavy metals. Biosorption of metals by the algal biomass followed by the recovery achieves four aims: firstly, improving quality of water resources and elimination of the environmental pollution, secondly recovery of the removed metals, thirdly let the algal biomass application is not for one use but is used for many times till four cycles of sorption-desorption with a reasonable capacity, and fourthly secure the final getting rid of the algal biomass after exhaustion, as the further decomposition of died algal biomass will not lead to release of the metals again into the environment.

Acknowledgements Special gratitude is expressed to sewage Company of Alexandria and New Borg El-Arab city Authority for sincere help and cooperation.

References

Abdullah SB (2010) Heavy metals removal from industries wastewater by using seaweed through biosorption process. Ph.D. Thesis, Faculty of Civil Engineering & Earth Resources, University Malaysia Pahang, Malaysia

Abo-El Ela SI, Nawar SS (1980) Treatment of wastewater from an oil and soap factory via dissolved air flotation. Environ Inter 4:47–52

Aboulsoud YIEM (2008) Removal of certain heavy metals by biomaterials derived from some Egyptian algae. M.Sc. Thesis, Faculty of Science, Ain Shams University, Egypt

Ahalya N, Ramachandra TV, Kanamadi RD (2003) Biosorption of heavy metals. Res J Chem Environ 7:71–79

Aksu Z (2002) Determination of the equilibrium, kinetic and thermodynamic parameters of the batch biosorption of nickel(II) ions onto *Chlorella vulgaris*. Process Biochem 38:89–99

Aksu Z (2005) Application of biosorption for the removal of organic pollutants: a review. Process Biochem 40:997–1026

Aleem AA (1993) Marine algae of Alexandria, Egypt. 138 pp., 55 plates

Arief VO, Trilestari K, Sunarso J, Indraswati N, Ismadji S (2008) Recent progress on biosorption of heavy metals from liquids using low cost biosorbents: characterization, biosorption parameters and mechanism studies. Clean 36:937–962

Bakatula EN, Cukrowska EM, Weiersbye IM, Mihaly-Cozmuta L, Peter A, Tutu H (2014) Biosorption of trace elements from aqueous systems in gold mining sites by the filamentous green algae (*Oedogonium* sp.) J Geochem Explor 144:492–503

Bisschops I, Spanjers H (2003) Literature review on textile wastewater characterization. Environ Technol 24:1399–1411

Bulgariu L, Bulgariu D (2014) Enhancing biosorption characteristics of marine green algae (*Ulva lactuca*) for heavy metals removal by alkaline treatment. J Bioprocess Biotech 4:146

Davis TA, Volesky B, Mucci A (2003) A review of the biochemistry of heavy metal biosorption by brown algae. Water Res 37:4311–4330

Deng L, Su Y, Su H, Wang X, Zhu X (2006) Biosorption of copper (II) and lead (II) from aqueous solutions by nonliving green algae *Cladophora fascicularis*: equilibrium, kinetics and environmental effects. Adsorption 12:267–277

Doner G, Ege A (2004) Evaluation of digestion procedures for the determination of iron and zinc in biscuits by flame atomic absorption spectrometry. Analyt Chim Acta 520:217–222

Elrefaii AH, Sallam LA, Hamdy AA, Ahmed EF (2012) Optimization of some heavy metals biosorption by representative Egyptian marine algae. J Phycol 48:471–474

Fakhry EM (2013) *Padina pavonica* for the removal of dye from polluted water. Am J Plant Sci 4:1983–1989

Farah JY, El-Gendy NS (2013) Performance, kinetics and equilibrium in biosorption of anionic dye acid red 14 by the waste biomass of *Saccharomyces cerevisiae* as a low-cost biosorbent. Turkish J Eng Env Sci 37:146–161

Faremi AY, Oloyede OB (2010) Biochemical assessment of the effects of soap and detergent instrumental effluents on some enzymes in the stomach of albino rats. Res J Environ Toxicol 4:127–133

Figueira MM, Volesky B, Mathieu HJ (1999) Instrumental analysis study of iron species biosorption by *Sargassum* biomass. Environ Sci Technol 33:1840–1846

Figueira MM, Volesky B, Ciminelli VST, Roddick FA (2000) Biosorption of metals in brown seaweed biomass. Water Res 34: 196–204

Goettsche R, Reuther W (1993) Wood preservative based on polymeric nitrogen compounds and metal-fixing acids. US Patent 5:186,947

He J, Chen PJ (2014) A comprehensive review on biosorption of heavy metals by algal biomass: materials, performances, chemistry, and modeling simulation tools. Bioresour Technol 160:67–78

Hussein RA, El-Sebaie OD, El-Sharkawy FM, Mahmoud AH, Ramadan MH (2005) Assessment of the waste stabilization pond performance, new Borg el-Arab city. JEPHAss 80:1–25

Jones RW (2000) Infrared technology, vol 14, ECT 4th edn. Ames Laboratory, United States Department Of Energy (USDOE), Washington, pp 379–416

Kanwal F, Rehman R, Mushtaq MW, Batool A, Naseem S (2013) Use of *Opuntia dillenii* seeds for sorptive removal of acidic textile dyes from water in benign way. Asian J Chem 25:7710–7714

Kulekci MK (2008) Magnesium and its alloys applications in automotive industry. Int J Adv Manuf Technol 39:851–865

Kumar KV, Sivanesan S, Ramamurthi V (2005) Adsorption of malachite green onto *Pithophora* sp., a fresh water algae: equilibrium and kinetic modeling. Process Biochem 40:2865–2872

Liu Y, Cao Q, Luo F, Chen J (2009) Biosorption of Cd^{2+}, Cu^{2+}, Ni^{2+} and Zn^{2+} ions from aqueous solutions by pretreated biomass of brown algae. J Hazard Mater 163:931–938

Natarajan ST, Jayaraj R, Thanaraj PJ, Prasath PMD (2011) The removal of heavy metal chromium (VI) from aqueous solution by using marine algae *Gracilaria edulis*. J Chem Pharm Res 3:595–604

Orme J, Ohanian E (1990) Assessing the health risks of aluminum. Environ Geochem Health 12:55–58

Rozic M, Macefat MR, Orescanin V (2005) Elemental analysis of ashes of office papers by EDXRF spectrometry. Nucl Instru Meth Physics Res B 229:117–122

Saibaba NKV, King P (2013) Equilibrium and thermodynamic studies for dye removal using biosorption. IMPACT: IJRET 1(3):17–24

Salima A, Benaouda B, Noureddine B, Duclaux L (2013) Application of *Ulva lactuca* and *Systoseira stricta* algae-based activated carbons to hazardous cationic dyes removal from industrial effluents. Water Res 47:3375–3388

Sarı A, Tuzen M (2009) Equilibrium, thermodynamic and kinetic studies on aluminum biosorption from aqueous solution by brown algae (*Padina pavonica*) biomass. J Hazard Mater 171:973–979

Shukla PM, Shukla SR (2013) Biosorption of cu(II), Pb(II), Ni(II), and Fe(II) on alkali treated coir fibers. Sep Sci Technol 48:421–428

Smith E, Wang J, Wang X, Jiang C (2012) Bar soap comprising pyrithione sources. US Patent Appl 2012/0220516A1

Straley JM, Fisher JG (1959) Metallizable Azo dyes prepared from a benzothiazole derivative and β-naphthol. US Patent 2:875,190

Strugariu ML, Heput T (2012) Monitoring results on industrial wastewater pollutants in steel industry. Acta Technica Corviniensis- Bulletin of Engineering, Faculty of Engineering, Hunedoara, Romania, October–December 33–36

Sud D, Mahajan G, Kaur MP (2008) Agricultural waste material as potential adsorbent for sequestering heavy metal ions from aqueous solutions - a review. Bioresour Technol 99:6017–6027

Tamilselvan N, Hemachandran J, Thirumalai T, Sharma VC, Kannabiran K, David E (2013) Biosorption of heavy metals from aqueous solution by *Gracilaria corticata varcartecala* and *Grateloupia lithophila*. JCLM 1:102–107

Tisler T, Koncan JZ (1999) Toxicity evaluation of wastewater from the pharmaceutical industry to aquatic organisms. Water Sci Tech 39: 71–76

Tüzün İ, Bayramoğlu G, Yalçın E, Başaran G, Çelik G, Arıca MY (2005) Equilibrium and kinetic studies on biosorption of hg(II), cd(II) and Pb(II) ions onto microalgae *Chlamydomonas reinhardtii*. J Environ Manag 77:85–92

Vilar VJP, Botelho CMS, Boaventura RAR (2005) Influence of pH, ionic strength and temperature on lead biosorption by *Gelidium* and agar extraction algal waste. Process Biochem 40:3267–3275

Vitali D, Dragojevic IV, Sebecic B (2008) Bioaccessibility of Ca, mg, Mn and cu from whole grain tea-biscuits: Impact of proteins, phytic acid and polyphenols. Food Chem 110:62–68

Vitor V, Corso CR (2008) Decolorization of textile dye by *Candida albicans* isolated from industrial effluents. J Ind Microbiol Biotechnol 35:1353–1357

Waller RA, Duncan DB (1969) A Bayes rule for the symmetric multiple comparisons problem. J Amer Stat Assoc 64:1484–1503

Wells AF (1975) Structural inorganic chemistry, 4th edn. Oxford Univ. Press, Oxford **259p**

WQA (Water Quality Association) (2013) National primary drinking water standards and treatment methods. [Online], Retrieved March 1, 2013, from http://www.wqa.org/consumer/alltables.cfm?SubTitleID=1&MainTitleID=1

Xu G, Goodell B (2001) Mechanisms of wood degradation by brown-rot fungi: chelator-mediated cellulose degradation and binding of iron by cellulose. J Biotechnol 87:43–57

Yoshio S, Tadashi F (1995) Skin cosmetics. European Patent. EP0612516

Zinova AD (1967) Key of green, brown and red algae of southern seas of USSR. Prin. Nauka Acad. Nauk USSR, 310pp